UDC 621.373.8: 621.375.826

Long-wavelength Semiconductor Lasers on InGaAs Ternary Substrates with Excellent Temperature Characteristics

●Koji Otsubo ●Yoshito Nishijima ●Hiroshi Ishikawa

(Manuscript received June 4,1998)

This paper proposes the use of InGaAs ternary bulk substrates as a technical breakthrough in long-wavelength semiconductor lasers. Deep-potential and large optical gain quantum wells fabricated on these substrates are expected to have excellent temperature characteristics, for example, a high characteristic temperature (T_0), temperature-insensitive efficiency, and high-temperature operation. The multi-component zone growth method has made InGaAs substrates having a high indium content possible. Fabricated edge-emitting lasers have lased at 1.23 µm with a record high T_0 of 140 K and a high lasing temperature of 210°C. Suppression of carrier overflow due to the deep potential wells is experimentally indicated by the small temperature dependence (–0.0051 dB/K) of the slope efficiency. The threshold current density must be reduced in order to obtain a much better temperature durability. The application of InGaAs substrates to long-wavelength vertical cavity surface emitting lasers (VCSELs) is also discussed.

1. Introduction

The application of 1.3 µm semiconductor lasers having excellent temperature characteristics in future optical interconnections and optical subscriber loop systems is attracting much attention. The threshold current and emission efficiency of conventional InGaAsP/InP lasers on InP substrates strongly depend on operating temperature. The threshold current of a semiconductor laser increases with temperature by a factor of $\exp(T/T_0)$, where T_0 is the characteristic temperature and is used for evaluating the temperature characteristics of a semiconductor laser. The T_0 of conventional InGaAsP/InP lasers is typically between 50 K and 70 K. To realize coolerless, low-cost, and low-power-consumption optical interconnections and subscriber systems, 1.3 µm lasers having temperature-insensitive characteristics with a T_0 over 150 K are required. Compared to the InP-based lasers, 0.98 µm InGaAs/GaAs lasers on GaAs substrates have shown a T_0 of over 200 K. The difference in temperature characteristics between long-wavelength InP-based lasers and 0.98 µm GaAs-based lasers had been a riddle for a long time until Ishikawa et al. studied the difference in the potential depth of the quantum wells used in the active layers of these lasers.[1),2)] **Figure 1** shows the band diagrams and refractive index distributions of the quantum wells. In shallow potential

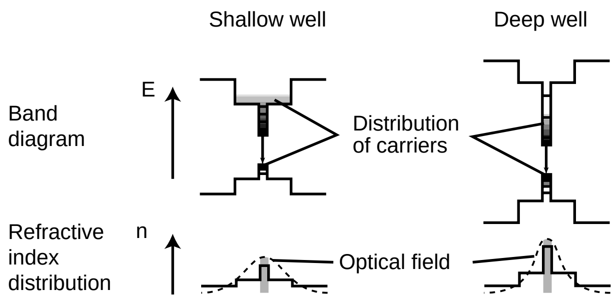

Figure 1
Band diagrams and refractive index distributions of shallow and deep quantum wells.

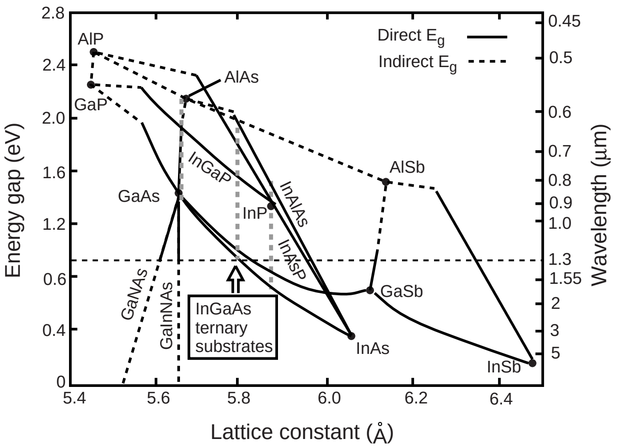

Figure 2
Bandgap energy versus lattice constant of III-V compound semiconductors.

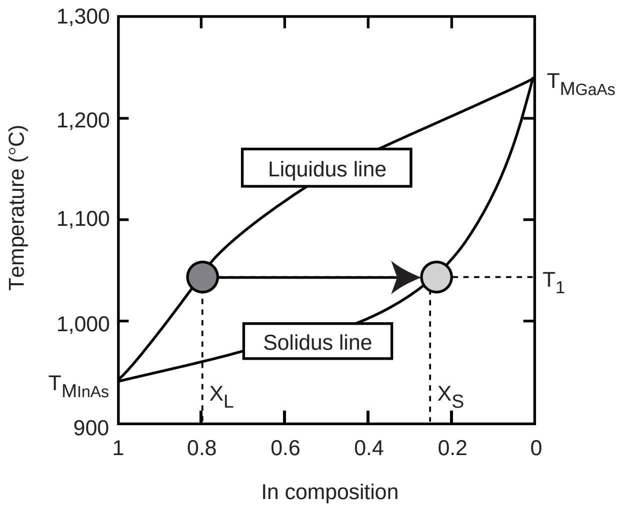

Figure 4
Pseudobinary phase diagram of InAs and GaAs.

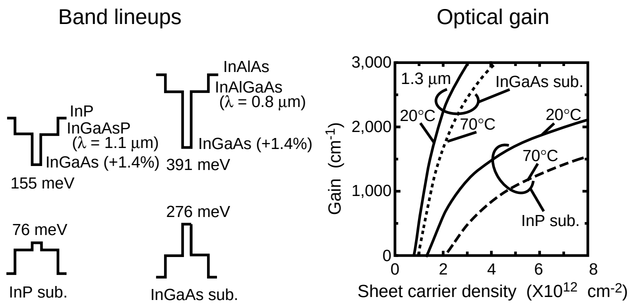

Figure 3
Band lineups of 1.3 μm quantum wells on InP substrates, and InGaAs substrates and their calculated optical gain.

wells like those of the InP-based lasers, carriers easily disperse to higher quantum levels and overflow to the barrier layers. By deepening the wells, more carriers are confined to the lowest quantum level, thus preventing overflow to the barrier layers, as is the case in the GaAs-based 0.98 μm lasers. Deep potential quantum wells are also advantageous in optical confinement. This explains why larger optical gains are expected in deep potential quantum wells and also explains the difference in temperature characteristics between InGaAsP/InP lasers and 0.98 μm InGaAs/GaAs lasers.

Realizing deep-potential quantum wells emitting at 1.3 μm should improve the temperature characteristics in 1.3 μm semiconductor lasers. We have proposed the use of InGaAs ternary substrates. **Figure 2** shows the bandgap energy versus the lattice constant of III-V compound semiconductors. Compressively-strained 1.3 μm quantum wells with wider bandgap barrier layers of materials such as InAlGaAs and InGaAsP can be grown on InGaAs ternary substrates whose indium composition is between 0.25 and 0.3. **Figure 3** shows the band lineups of 1.3 μm quantum wells on InP substrates and InGaAs substrates and their calculated optical gains.[1),2)] Carrier overflow to the separate confinement heterostructure (SCH) layers is taken into account in the calculations. The deeper potential wells on InGaAs substrates gives a larger optical gain and smaller temperature dependence than those on InP substrates, owing to suppression of carrier overflow. After our proposal of utilizing deep-potential wells for improving the temperature characteristics, several technical approaches have also been studied to realize deep wells emitting in the long wavelength region.[3)-6)]

In this work, we fabricated long-wavelength strained quantum well lasers on InGaAs ternary substrates. Our process and the results of fabricating InGaAs ternary substrates are described in Chapter 2. In Chapter 3, the characteristics of the strained quantum well lasers on the InGaAs

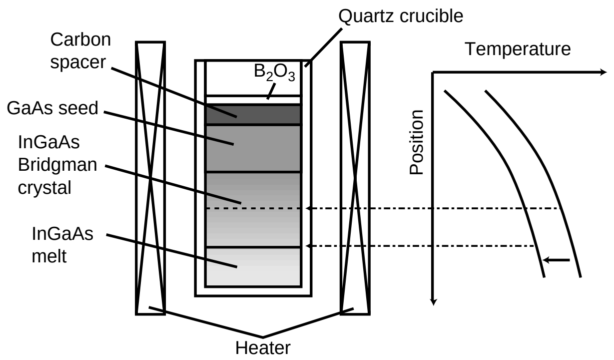

Figure 5
Bridgman growth method.

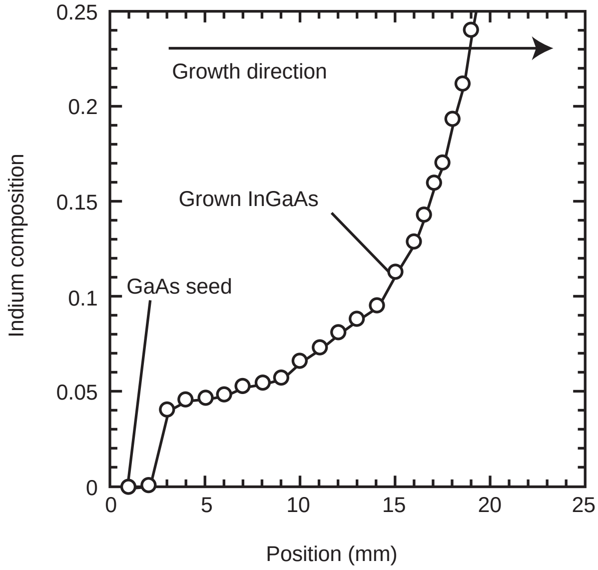

Figure 6
Distribution along growth direction of indium composition of Bridgman-grown InGaAs crystal.

substrates are presented. In Chapter 4, we touch on the application of InGaAs ternary substrates to low-voltage-driven 1.3 µm vertical cavity surface emitting lasers (VCSELs). Finally, the conclusions are given in Chapter 5.

2. Fabrication of InGaAs Ternary Substrates

Until now, InP and GaAs substrates have been used for long-wavelength semiconductor lasers. We started our research by growing InGaAs bulk crystals in-house to obtain the ternary substrates. Binary bulk crystals such as GaAs and InP are grown by cooling their growth system. However, when it comes to the crystal growth of ternary semiconductors, the process is not so simple. **Figure 4** shows the pseudobinary phase diagram of InAs and GaAs. When we grow compositionally uniform InGaAs bulk crystals with an indium content of X_S, we must keep the temperature of the growing interfaces at T_1 and supply GaAs as a driving force. We grew the InGaAs bulk crystals with an indium content of up to 0.1 using the liquid encapsulated Czochralski (LEC) method.[7] InGaAs having an indium content greater than 0.2 is extremely difficult to grow by the LEC method. With such a content, the separation of the solidus and liquidus lines becomes very large and the source is consumed so much that the required temperature stability cannot be achieved.

We are trying to grow InGaAs substrates with a higher indium content by a new multi-component zone growth method[8),9)] in which the InGaAs crystals grown by the Bridgman method are used as seed crystals.[9),10)] **Figure 5** outlines the Bridgman method. In this method, InGaAs crystals are grown simply by heating and cooling the system. Compositionally graded InGaAs single crystals and InGaAs melts are formed by the growth. **Figure 6** shows the indium composition of the Bridgman-grown InGaAs crystal as determined by energy-dispersive X-ray (EDX) analysis. We have established the conditions for growing single InGaAs crystals having an indium composition of around 0.25 with good reproducibility.[9)] However, as shown in Figure 6, the gradient of indium composition against the growth direction is so steep in the region of high indium content that much of the substrate is not available for growth. $In_xGa_{1-x}As$ ($x > 0.25$) crystals which are compositionally uniform along the growth direction are required to obtain large numbers of substrates of good quality. The modified multi-component zone growth is suitable for this purpose. In this method, the InGaAs seed and melt grown by the Bridgman method and the GaAs source crystals are set as shown in **Figure 7**.[9)] When the whole system is kept at the temperature distribution shown on the right in Figure 7, InGaAs crystals grow on the InGaAs seed crystals. InGaAs crystals with a uniform indium composition can be grown by cooling the system while keeping the temperature of the growing interface constant and supplying GaAs as the driving force. Temperature control at the growth interface becomes easier because the whole setup is smaller than that of the LEC method. Recent results of the multi-component zone growth method are described in Ref. 9. We expect that optimizing the crystal growth conditions will enable us to grow single and uniform zone-grown crystals having an indium composition of over 0.25.

We sliced the Bridgman-grown bulk crystals into substrates along the (100) direction. Surface dicing damage was removed by wet chemical etching. To investigate the quality of the $In_{0.22}Ga_{0.78}As$ substrate, we compared its full width at half maximum in an X-ray rocking curve with that of a commercial GaAs substrate; the results are shown in **Figure 8**. The value of 490 seconds for the InGaAs substrate is more than 20 times larger than that of the GaAs substrate. **Figure 9** compares reciprocal space maps of the InGaAs and GaAs substrates. The X-ray intensity distribution of the InGaAs substrate broadens along the x-direction and is wider than that of the GaAs

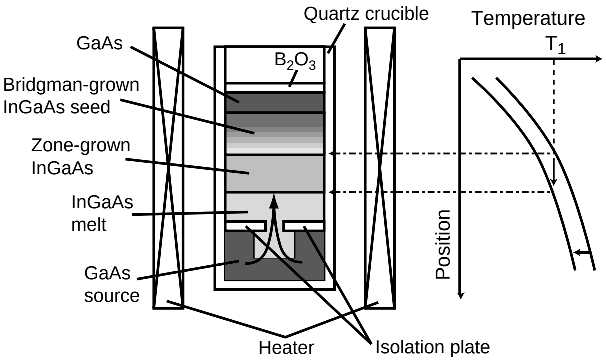

Figure 7
New multi-component zone growth method.

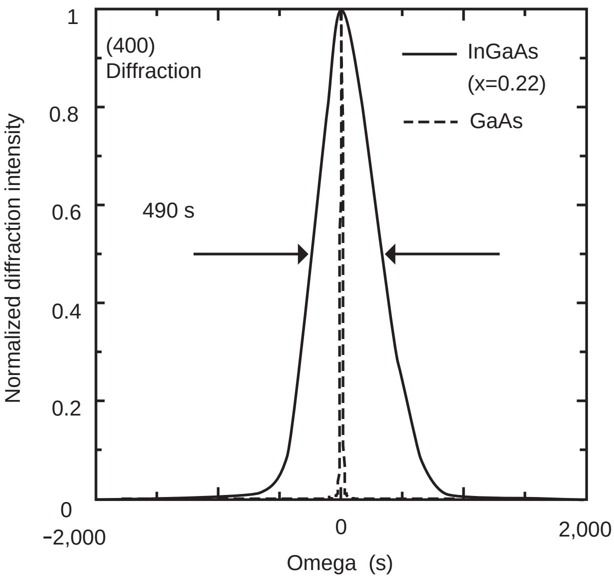

Figure 8
X-ray rocking curves of InGaAs substrate and commercial GaAs substrate.

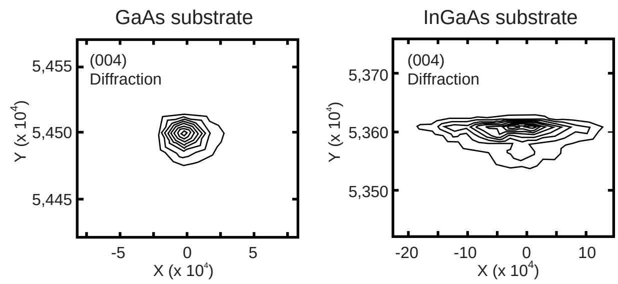

Figure 9
Reciprocal space maps of InGaAs substrate and GaAs substrate.

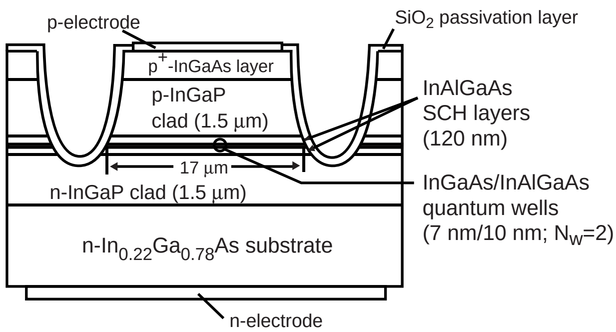

Figure 10
Schematic cross section of fabricated laser.

substrate. No other signals are found in the map of the InGaAs substrate. This means that the main causes of the broadening in the rocking curve is not fluctuation in the lattice constant but fluctuation in the orientation of the crystal axis. Although we could have made further improvements to the quality of the substrates, we went ahead and fabricated lasers to examine the feasibility of the grown InGaAs substrates.

3. Strained Quantum Well Lasers on InGaAs Substrates

3.1 Fabrication

Figure 10 shows a schematic cross section of the fabricated lasers. The double heterostructure was grown on the Bridgman-grown n-$In_{0.22}Ga_{0.78}As$ substrates by metalorganic vapor phase epitaxy (MOVPE) and consists of an n-InGaP cladding layer (1.5 μm), an undoped double-quantum-well active layer sandwiched by 120 nm-thick InAlGaAs separate confinement heterostructure (SCH) layers, a p-InGaP cladding layer (1.5 μm), and a highly p-doped InGaAs contact layer (0.5 μm). The quantum wells consist of two 7 nm-thick $In_{0.41}Ga_{0.59}As$ 1.32%-compressively-strained wells separated by a 10 nm-thick InAlGaAs barrier layer. The maximum gain of the well layers was adjusted in the 1.2 μm region because the indium content of the substrate is 0.22, which is not enough to fabricate 1.3 μm lasers. The compositional wavelength of the InAlGaAs layers in the structure was set at 0.9 μm in order to make deep-potential wells. Mesa stripes for carrier and optical confinement were defined by wet chemical etching. The width of the active layers was 17 μm. Electrodes were formed on the p-InGaAs layer and the InGaAs substrate. In some samples, 95% high-reflectivity (HR) layers were deposited on both facets. The laser chips were bonded on diamond heatsinks with the junction-side down.

3.2 Experimental results

Figure 11 shows the temperature dependence of light output versus current of the 600 μm-long laser with HR-coated facets under pulsed operation. The pulse width was 500 ns and the repetition rate was 1 kHz. The threshold current at 20˚C was 25 mA, and the corresponding threshold current density was 245 A/cm^2. The lasing wavelength was 1.226 μm at 20˚C, and the characteristic temperature (T_0) between 20˚C and 50˚C

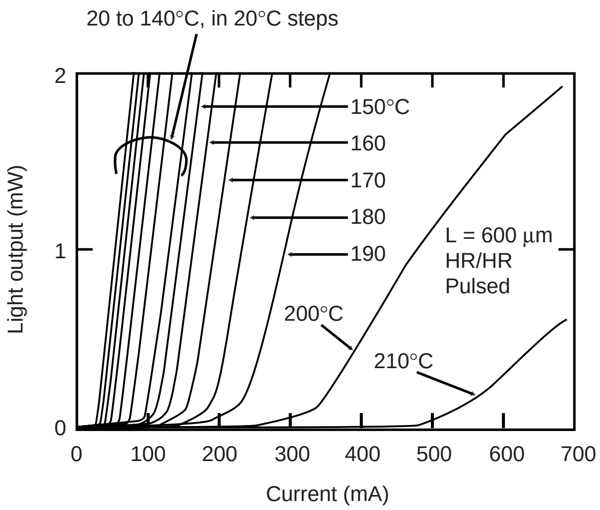

Figure 11
Temperature dependence of light output versus current. Lasing occurs up to 210˚C.

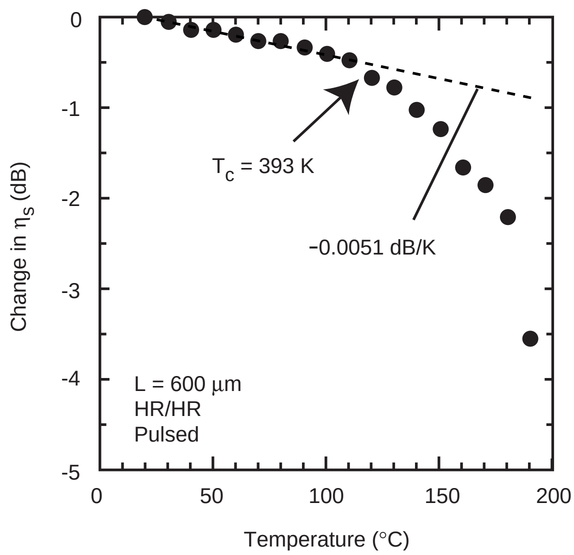

Figure 12
Temperature dependence of change in η_s from η_s at 20˚C. Temperature sensitivity of η_s below 393 K (120˚C) is −0.0051 dB/K.

was 110 K. Lasing up to 210°C was observed.[11] It is clearly seen from Figure 11 that the slope efficiency (η_s) is almost independent of the operating temperature over a wide temperature range. The reduction of η_s from the value at 20°C for various temperatures is shown in **Figure 12**. The critical temperature (T_c) defined by Seki et al., [12] where the rate of reduction of the slope efficiency becomes larger, is 393 K. The temperature sensitivity below T_c is as low as -0.0051 dB/K. The T_c and temperature sensitivity of η_s indicate the reduction of optical loss associated with reduced carrier overflow to the SCH layers.[12] This laser also lases under continuous wave (CW) operation. **Figure 13** shows the temperature dependence of CW light output versus current. The maximum output power of this sample is over 10 mW, while that of an as-cleaved sample exceeds 50 mW. The sample's electrical resistance is 2.3 ohms, which is high for the size of its injected area. A further improvement of the temperature characteristics under CW operation could be realized by optimizing the layer structure. The temperature dependence of the threshold current density of the sample with the lowest threshold, which was as low as 176 A/cm^2 at 20°C, is shown in **Figure 14**. A record high T_0 of 140 K was achieved.[13] Even though there were only two quantum wells, the lasers exhibited superior temperature characteristics. The grown crystal showed poor surface morphology, and we believe that optical scattering loss induced by the poor morphology still remains in these lasers and a much lower threshold and better temperature characteristics can be achieved by improving the quality of the InGaAs substrates.

The dependence of the characteristic temperature on the threshold current density per well is shown in **Figure 15**.[14),15] A temperature-insensitive slope efficiency was observed even in the high-threshold samples with characteristic temperatures of below 80 K. This suggests that carrier overflow to the SCH layers is suppressed in all of these InGaAs-based lasers. As we found with the InP-based laser, the lower the threshold, the higher the characteristic temperature. This dependence is stronger in the InGaAs-based laser than in the InP-based one. We presume that, in the

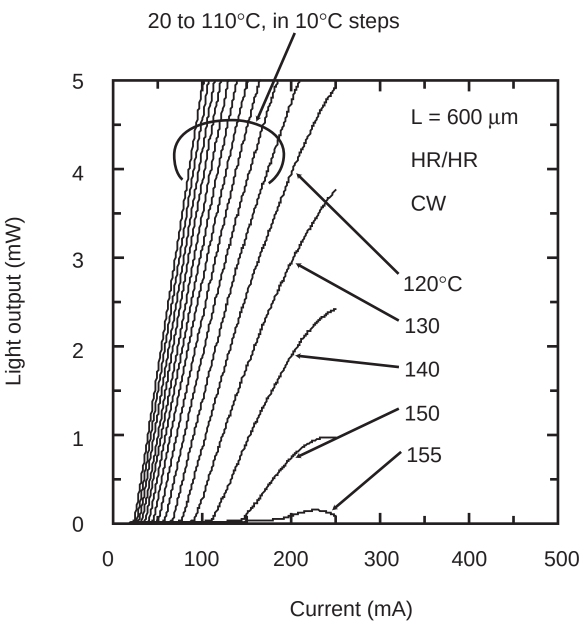

Figure 13
Temperature dependence of CW light output versus current.

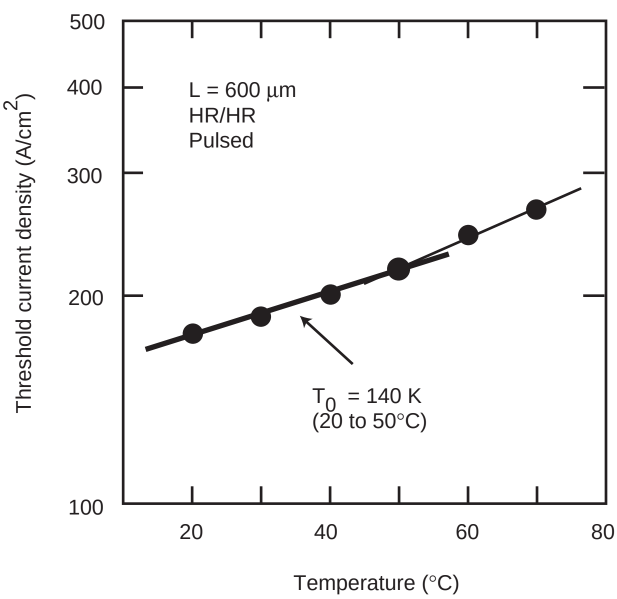

Figure 14
Temperature dependence of threshold current density of sample with lowest threshold. T_0 between 20 and 50°C is 140 K.

InGaAs-based laser, in which we can neglect the effect of carrier overflow, this stronger dependence reflects Auger nonradiative recombination, which has a cubic dependence on carrier density. In the InP-based laser, carrier overflow weakens the dependence. Further investigations should be carried out in order to clarify the dominant influence on the characteristic temperature. As seen in Figure 15, we believe that a much better temperature durability can be obtained even in as-cleaved lasers by reducing the threshold current density, which will be realized by increasing the number of quantum wells.

4. Application to 1.3 μm Vertical Cavity Surface Emitting Lasers (VCSELs)

Vertical cavity surface emitting lasers (VCSELs) emit light parallel to the growth direction of double heterostructures; this is in contrast to edge emitting lasers, which emit perpendicularly to the crystal growth direction. Most VCSELs consist of high-reflectivity (>95%) multi-stacked distributed Bragg reflector (DBR) mirrors and cavities having an optical length that is several times that of the light's wavelength. Therefore, their volume is much smaller than that of stripe lasers. VCSELs are also attractive devices for optical interconnection systems for the following reasons. An extremely low threshold of several microamperes is expected due to the small volume of their active regions. Two-dimensional arrays are feasible because they no longer need cleaved facets. The light emitting area of VCSELs is larger than that of edge emitting lasers, so coupling to optical fibers becomes easier. Although superior characteristics have been reported for 0.98 μm GaAs-based VCSELs[16], long-wavelength VCSELs with practical characteristics have not yet been realized. Because 1.3 μm VCSELs operate at a longer wavelength, they have a lower built-in voltage and therefore a lower driving voltage. This should make it possible to drive them directly with CMOS.

Chapter 3 presented experimental result which proved the merit of deep-potential and large optical gain quantum wells on InGaAs ternary substrates in edge emitting lasers. When they are applied to long-wavelength VCSELs, there is another advantage over long-wavelength VCSELs on InP substrates[17),18] and those fabricated using the

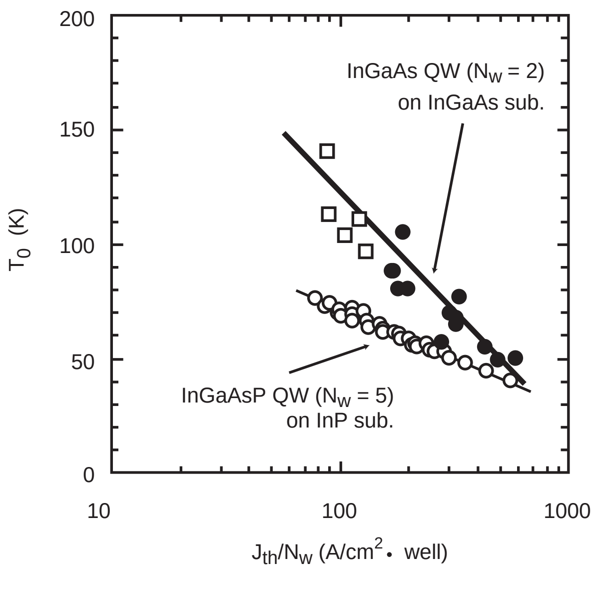

Figure 15
Dependence of characteristic temperature on threshold current density per well. Black circles are for as-cleaved lasers and squares are for HR-coated lasers.

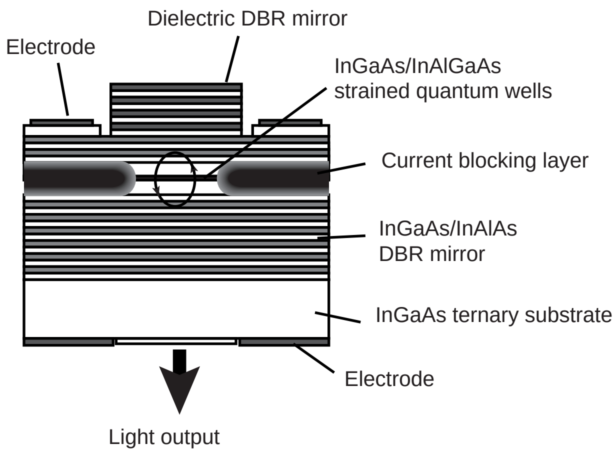

Figure 16
Schematic cross section of proposed VCSEL on InGaAs substrates.

wafer fusion technique.[19] High-reflectivity DBR mirrors, which are essential for high-performance, long-wavelength VCSELs, can be epitaxially grown on the InGaAs ternary substrates together with the large optical gain quantum wells. **Figure 16** shows a schematic cross section of the proposed VCSEL on InGaAs substrates. The InGaAs/InAlAs system is chosen for the semiconductor DBR mirrors. The large difference in the refractive indexes of the mirror materials makes the reflectivity high. The best semiconductor material system for DBR mirrors is GaAs/AlAs, which gives a refractive index difference of 0.503; the difference between InGaAs and InAlAs lattice-matched to the InGaAs substrates is 0.418, which is double that of the InP/InGaAsP system. **Figure 17** shows the calculated reflectivity of the InP/InGaAsP mirrors on InP substrates and the InGaAs/InAlAs mirrors on InGaAs substrates.[20),21)] It is very clear that a high reflectivity of over 99.5% can be obtained with fewer pairs in the ternary system we proposed. We previously fabricated InGaAs/InAlAs DBR mirrors on quasi-InGaAs-substrates, that is, InGaAs compositionally-graded buffer layers on GaAs substrates.[21)] Figure 17 also shows the measured pair-dependence of reflectivity. The experimental results agree quite well with the calculated reflectivity up to 10 pairs. When the number of pairs exceeds 10, a discrepancy between the experimental and calculated reflectivity is observed, which is due to enhanced surface roughness resembling a crosshatched pattern. This problem should be overcome by fabricating the mirrors on InGaAs ternary substrates. **Figure 18** shows the calculated dependence of threshold current density on the mean reflectivity of DBR mirrors.[20)] As shown in Figure 17, a large number of pairs is required to obtain a reflectivity of over 99% in InP/InGaAsP mirrors and it is extremely difficult and unrealistic to grow them. When InGaAs/InAlAs DBR mirrors are grown on InGaAs substrates, those having 25 pairs can achieve a reflectivity of over 99.5%, which is why a drastic reduction of threshold current is expected in the VCSELs on InGaAs ternary substrates. In this way, high-performance 1.3 µm VCSELs should be realized on InGaAs ternary substrates.

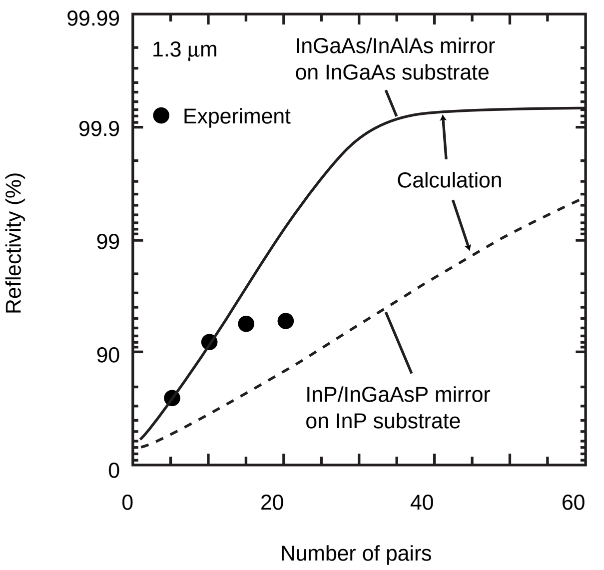

Figure 17
Calculated reflectivity of InP/InGaAsP mirrors on InP substrates and InGaAs/InAlAs mirrors on InGaAs substrates. Black circles show measured reflectivity of InGaAs/InAlAs mirrors grown on InGaAs graded buffer layers.

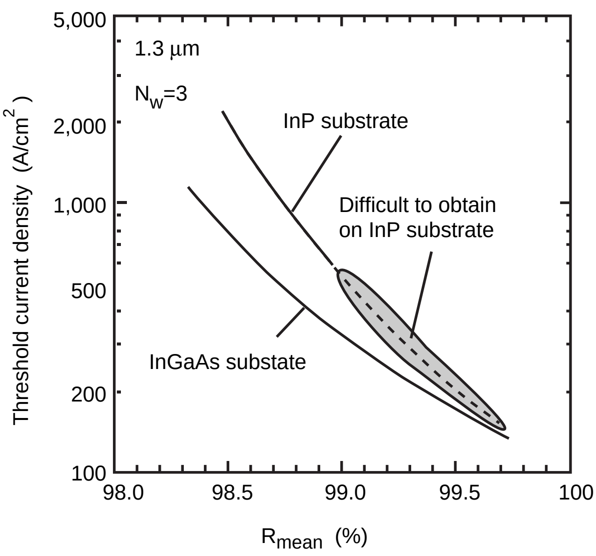

Figure 18
Calculated dependence of threshold current density on mean reflectivity of DBR mirrors.

5. Conclusion

This paper proposed the use of InGaAs ternary substrates as a way to improve the temperature performance in long-wavelength semiconductor edge-emitting lasers and VCSELs. The $In_xGa_{1-x}As$ ternary substrates (X>0.25) should enable the realization of high-performance 1.3 µm strained quantum well lasers. We have established the Bridgman-growth conditions for single InGaAs bulk crystals having an indium composition of around 0.2, and have introduced the new multi-component zone growth technique for InGaAs substrates having a higher indium content. Fabricated strained double quantum well lasers emitting in the 1.2 µm region showed an excellent temperature durability, for example, a record high T_0 of 140 K, a high lasing temperature of 210˚C, and a slope efficiency with a temperature sensitivity of only –0.0051 dB/K. Also, it should be possible to fabricate high-performance long-wavelength VCSELs on InGaAs ternary substrates by combining large optical gain quantum wells with high-reflectivity InGaAs/InAlAs DBR mirrors. Fabrication of semiconductor lasers on $In_xGa_{1-x}As$ ($x > 0.25$) substrates should enable 1.3 µm lasing and superior temperature characteristics. If such characteristics are obtained in 1.3 µm semiconductor lasers on InGaAs ternary substrates, they will be candidate components of coolerless, low-cost, and low-power-consumption optical interconnection and subscriber systems.

Acknowledgments

Some parts of this work were carried out in the Optical Interconnection Fujitsu Laboratory, Real World Computing Partnership. The authors thank Dr. H. Shoji, Mr. T. Kusunoki, Dr. T. Suzuki, Mr. T. Uchida, Dr. T. Fujii, and Dr. K. Nakajima of Fujitsu Laboratories Ltd. for their contribution to this work and the fruitful discussions we had with them.

References

1) H. Ishikawa: Theoretical gain of strained quantum well grown on InGaAs ternary substrate. *Appl. Phys. Lett.*, **63**, pp.712-714 (1993).
2) H. Ishikawa and I. Suemune: Analysis of temperature dependent optical gain of strained quantum well taking account of carriers in the SCH layer. *IEEE Photon. Technol. Lett.*, **6**, pp.344-347 (1994).
3) C-E. Zah, R. Bhat, B. N. Pathak, F. Favire, W. Lin, M. C. Wang, N. C. Andreadakis, D. M. Hwang, M. A. Koza, T-P. Lee, Z. Wang, D. Darby, D. Flanders, and J. J. Hsieh: High-performance uncooled 1.3-µm $Al_xGa_yIn_{1-x-y}As$/InP strained-layer quantum-well lasers for subscriber loop applications. *IEEE J. Quantum Electron.*, **30**, pp.511-523 (1994).
4) M. Kondow, K. Uomi, A. Niwa, T. Kitatani, S. Watahiki, and Y. Yazawa: GaInNAs: A novel material for long-wavelength-range laser diodes with excellent high-temperature performance. *Jpn. J. Appl. Phys.*, **35**, pp.1273-1275 (1996).
5) H. Oohashi, S. Seki, T. Hirono, H. Sugiura, T. Amano, M. Ueki, J. Nakano, M. Yamamoto, Y. Tohmori, M. Fukuda, and K. Yokoyama: High-power and high-efficiency 1.3 µm InAsP compressively-strained MQW lasers at high temperatures. *Electron. Lett.*, **31**, pp. 556-557 (1995).
6) T. Anan, M. Yamada, K. Tokutome, and S. Sugou: 1.3 µm InAsP/InAlGaAs MQW lasers for high-temperature operation. *Electron. Lett.*, **33**, 12, pp.1048-1049 (1997).
7) K. Nakajima and T. Kusunoki: Constant temperature LEC growth of InGaAs ternary bulk crystals using the double crucible method. *J. Crystal Growth*, **169**, pp.217-222 (1996).
8) T. Kusunoki, K. Nakajima, H. Shoji, and T. Suzuki: Growth of uniform InGaAs bulk crystal by multi-component zone melting method. *Mat. Res. Soc. Symp. Proc.*, **417**, pp.315-318 (1996).

9) Y. Nishijima, K. Nakajima, K. Otsubo, and H. Ishikawa: InGaAs bulk crystal growth for high T_0 semiconductor lasers. Conf. Proc. 1998 Int. Conf. InP & Related Materials, TuB1-5, Tsukuba, pp.45-48.
10) K. Nakajima, T. Kusunoki, and K. Otsubo: Bridgman growth of compositionally graded $In_xGa_{1-x}As$ (x = 0.05-0.30) single crystals for use as seeds for $In_{0.25}Ga_{0.75}As$ crystal growth. *J. Crystal Growth*., **173**, pp.42-50 (1997).
11) K. Otsubo, H. Shoji, T. Kusunoki, T. Suzuki, T. Uchida, Y. Nishijima, K. Nakajima, and H. Ishikawa: Long wavelength strained quantum well lasers oscillating up to 210˚C on InGaAs ternary substrates. *IEEE Photon. Technol. Lett*., **10**, 8, pp.1073-1075 (1998).
12) S. Seki, H. Oohashi, H. Sugiura, T. Hirono, and K. Yokoyama: Study on the dominant mechanisms for the temperature sensitivity of threshold current in 1.3-μm InP-Based strained-layer quantum-well lasers. *IEEE J. Quantum Electron*., **32**, 8, pp.1478-1486 (1996).
13) K. Otsubo, H. Shoji, T. Kusunoki, T. Suzuki, T. Uchida, Y. Nishijima, K. Nakajima, and H.Ishikawa: High T_0 (140 K) and low-threshold long-wavelength strained quantum well lasers on InGaAs ternary substrates. *Electron. Lett*., **33**, 21, pp.1795-1797 (1997).
14) H. Shoji, K. Otsubo, T. Kusunoki, T. Suzuki, T. Uchida, T. Fujii, Y. Nishijima, K. Nakajima, and H. Ishikawa: 1.3 μm semiconductor lasers on InGaAs ternary substrates toward low-threshold and temperature insensitive operation. Ext. Abstr. 1997 Int. Conf. Solid State Devices & Materials, C-1-1, Hamamatsu, pp.46-47.
15) H. Ishikawa: Present and prospects of high T_0 long-wavelength lasers on InGaAs ternary substrates. Tech. Dig. 1998 Conference on Lasers and Electro-Optics (CLEO '98), CWL3, San Francisco, CA, pp.293-294.
16) G. M. Yang, M. H. MacDougal, and P. D. Dapkus: Ultralow threshold current vertical-cavity surface-emitting lasers obtained with selective oxidation. *Electron. Lett*., **31**, 11, pp. 886-888 (1995).
17) T. Baba, Y. Yogo, Y. Suzuki, F. Koyama, and K. Iga: Near room temperature continuous wave lasing characteristics of GaInAsP/InP surface emitting laser. *Electron. Lett*., **29**, pp. 913-914 (1993).
18) S. Uchiyama, N. Yokouchi, and T. Ninomiya: Continuous-wave operation up to 36˚C of 1.3-μm GaInAsP/InP vertical-cavity surface-emitting lasers. *IEEE Photon. Technol. Lett*., **9**, 2, pp.141-142 (1997).
19) D. I. Babic, K. Streubel, R. P. Mirin, N. M. Margalit, J. E. Bowers, E. L. Hu, D. E. Mars, L. Yang, and K. Carey: Room-temperature continuous-wave operation of 1.54-μm vertical-cavity lasers. *IEEE Photon. Technol. Lett*., **7**, 11, pp.1225-1227 (1995).
20) H. Shoji, K. Otsubo, T. Fujii, and H. Ishikawa: Calculated performance of 1.3 μm vertical-cavity surface-emitting lasers on InGaAs ternary substrates. *IEEE J. Quantum Electron*., **33**, 2, pp. 238-245 (1997).
21) K. Otsubo, H. Shoji, T. Fujii, M. Matsuda, and H. Ishikawa: High-reflectivity $In_{0.29}Ga_{0.71}As$/ $In_{0.28}Al_{0.72}As$ ternary mirrors for 1.3 μm vertical-cavity surface-emitting lasers grown on GaAs. *Jpn. J. Appl. Phys*., **34**, 2B, pp.L227-229 (1995).

Koji Otsubo received a B.E.degree and an M.E.degree from Tohoku University, Sendai in 1989 and 1991, respectively. He joined Fujitsu Laboratories Ltd., Atsugi in 1991 and has been engaged in basic research of long-wavelength semiconductor lasers. Since 1992, he has also been at the RWCP Optical Interconnection Fujitsu Laboratory. He is a member of the Japan Society of Applied Physics (JSAP). In 1998, he jointly received the SSDM Paper Award with his collaborators and the JSAP Research Paper Presentation Award.

E-mail : kotsubo@flab.fujitsu.co.jp

Yoshito Nishijima received a B.E. degree from Tokyo Institute of Technology in 1974, an M.E. degree from Kyoto University in 1976, and a Dr. degree from Shizuoka University in 1995. He joined Fujitsu Laboratories Ltd., Akashi in 1976 and has been engaged in research and development of materials for infrared semiconductor lasers and detectors. He is a member of the Japan Society of Applied Physics. In 1998, he jointly received the SSDM Paper Award.

E-mail : nisijima@optsemi.atsugi.flab.fujitsu.co.jp

Hiroshi Ishikawa received the B.S. and M.E. degrees in Electronics from Tokyo Institute of Technology, Tokyo, Japan in 1970 and 1972, respectively. He joined Fujitsu Laboratories Ltd., Kawasaki in 1972 and has been engaged in the research and development of semiconductor lasers for optical communications. He received the Dr. degree from Tokyo Institute of Technology in 1984. He is a member of the Institute of Electronics, Information and Communication Engineers (IEICE) of Japan, the Japan Society of Applied Physics, the Optical Society of America, and a senior member of the Institute of Electrical and Electronics Engineers (IEEE). He received the Young Engineers Award in 1976 from the IEICE, the Invention Prize for Encouragement in 1990 from the Japan Institute of Invention and Innovation, and the SSDM Paper Award in 1998.

E-mail : ishikawa@flab.fujitsu.co.jp